

5G NR mmWave Indoor Coverage with Massive Antenna System

Syed Hassan Raza Naqvi, Pin Han Ho, and Limei Peng

Abstract: In this paper, we introduce a novel mmWave access architecture, called mmWave over cable (mmWoC), for achieving effective indoor coverage, which is characterized by using an analog modulated relay link to transport the outdoor mmWave signals to the indoors. To enable an effective mapping of radio signals on the cable sub-carriers, we introduce non-configurable air-to-cable (NC-A2C) scheduler that is characterized by its low control complexity and hardware requirement. We will discuss the merits of the proposed mmWoC access architecture and the NC-A2C scheduler, which are further validated via extensive simulations.

Index Terms: mmWave, mmWave indoor coverage, mmWave small cell (SC), mmWave wireless over cable (mmWoC).

I. INTRODUCTION

MILLIMETER Wave (mmWave) communication is an emerging 5G cellular technology aiming to meet the growing requirement on transmission rates and throughput. Particularly, the mmWave communication beyond 6 GHz has been employed in 5G NR and extensively investigated by international R&D organizations in both industry and academia for future cellular technology. Although with its extremely high bandwidth, mmWave communication suffers from high propagation losses due to penetration, reflection, and diffraction, thus causing reduced link budget as that in the scenario of sub-6 GHz. Such unique mmWave signal propagation characteristics have brought up new challenges, where innovative and viable solutions are required to take the best advantage of the high throughput capabilities in various application scenarios.

Massive small cells (SCs) deployment is considered a promising technique to improve the overall network capacity via high spectral reuse. In the cm-wave paradigm, the conventional approach for achieving connectivity between the base station (BS) and SCs, commonly referred to as backhaul link, is via optical fibers. Alternatively, mmWave links can be used to replace the optical fibers for achieving more flexible and cost effective deployment. The idea has been adopted by the integrated access

Manuscript received October 10, 2019; revised October 1, 2020; approved for publication by Young-Chai Ko, Division II Editor, November 4, 2020.

This research was supported by the BK21 FOUR project (AI-driven Convergence Software Education Research Program) funded by the Ministry of Education, School of Computer Science and Engineering, Kyungpook National University, Korea (4199990214394), and National Science and Engineering Research Council (NSERC), Canada.

S. H. R. Naqvi and P. H. Ho are with the Department of Electrical and Computer Engineering, University of Waterloo, ON, Canada, email: {shrnaqvi, p4ho}@uwaterloo.ca.

L. Peng is with the School of Computer Science and Engineering, Kyungpook National University, Daegu 41566, Korea, email: aurorapl@knu.ac.kr.

L. Peng is the corresponding author.

Digital Object Identifier: 10.23919/JCN.2020.000031

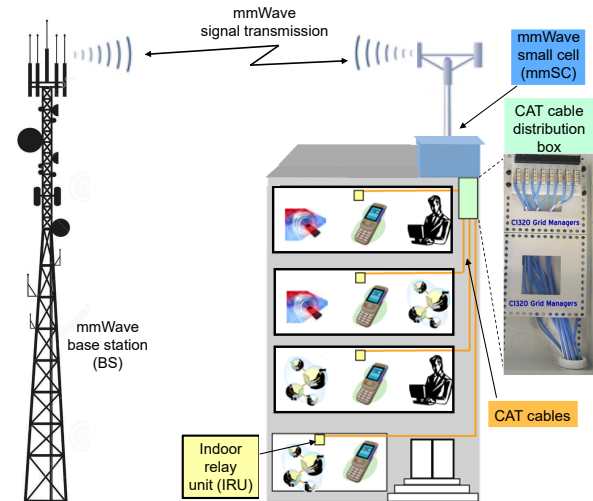


Fig. 1. 5G NR mmWave base station (BS) and small cell (mmSC) configuration for indoor coverage.

backhaul (IAB) project of 3GPP as a part of 5G NR standardization process [1], where in-band backhaul via mmWave links appears to be an attractive solution and gains extensive interest by the research community. In this case, the access links between user equipments (UEs) and SCs share the same radio spectrum with the backhaul links, where directional beamforming technique [2] can be used to effectively mitigate the inter-cell interference and high path loss.

To realize the IAB initiative of 3GPP, the paper investigates a novel access architecture for effective mmWave indoor coverage in the metropolitan area. An example is shown in Fig.1, where the mmWave small cell (mmSC) unit, deployed at the top of a building, works as an analog relay (or repeater) between the tower-mounted macro cell mmWave base station (mmBS) and the 5G NR UEs. In addition to the outdoor UEs, the proposed mmSC is connected with distributed indoor radio units (IRUs) via multi-pair LAN cables, so as to ensure line of sight (LOS) transmissions with the indoor UEs. Particularly, a single multi-pair cable (i.e., CAT 7) contains 4 twisted pairs and can provide up to a total throughput of more than 10 Gbps (for 100 m cable length) between an IRU and mmSC. Thus, the analog-modulated version of the mmWave signal is carried to each IRU that can well meet the targeted data rate of 5G.

The proposed mmWoC architecture for 5G indoor coverage yields the following merits:

- The design achieves an integrated outdoor and indoor service provisioning and is compatible with the conventional mmWave access network where an mmWave radio link connects an mmBS and an mmSC.

- The IRU is an all-analog and rate/protocol independent device without taking real-time configuration and dynamic control, which bears all the desired features for large-scale deployment.
- The proposed NC-A2C scheduler is novel by initiating a graceful compromise between the control/hardware complexity and total throughput.
- The use of multi-pair LAN cables (i.e., CAT 5/6/7) offers very cost effective solution as compared with new deployment of other type of wired media.

The rest of the paper is organized as follows. Section II reviews the prior arts on mmWave access for indoor coverage. Section III defines the proposed mmWoC access architecture that enables LOS transmissions for indoor UEs. System model is described in Section IV, where as the proposed NC-A2C scheduler is presented in Section V. Section VI examines the cable bundle characteristics and demonstrates the numerical results of the proposed NC-A2C scheduler. Section VII concludes the paper.

II. STATE-OF-THE-ART

A. Indoor Access Architecture

Identified by European Commission for 5G research in the Horizon 2020 project, the prime objective of 5G mobile systems is to achieve high spectral efficiency and ultra high data rate with low communication latency. The targeted 10 Gbps data rate for uplink (UL) and downlink (DL) is several folds larger than that in LTE-A Release 10, thanks to the employment of emerging technologies such as massive MIMO and small cells (SCs) in the mmWave spectrum.

The unique characteristic of mmWave channel characteristic and requirement of LOS transmission would cause significant difficulty in extending outdoor coverage into the indoor environment using the conventional mobile access architecture. Deployment of SCs by leveraging the mmWave spectrum beyond 6 GHz band seems to be a viable solution to ease the bandwidth demand. However, the conventional mobile access network architecture, particularly the backhaul links, is not capable of supporting the 5G data rates for indoor coverage, while the deployment of high speed access networks, such as fiber-to-the-home (FTTH), would be subject to prohibitively high cost [3].

Shared UE-side distributed antenna system (SUDAS) was proposed in [4], where the SUDAS indoor unit receives the signals from an outdoor macro BS on a licensed UHF band (referred as backend) that are relayed to the indoor users on mmWave spectrum (called frontend). Although SUDAS uses mmWave spectrum for indoor 5G coverage, the backend licensed UHF link becomes the bottleneck to achieve true 5G data rates. To improve spectral efficiency and extend 5G NR mmWave coverage for the non-LOS users, two-hop device-to-device (D2D) relay was proposed in [5], aiming to significantly reduce the deployment cost by taking idle UEs as relays. Although serving as a cost-effective approach, it can hardly serve as a 5G NR solution since the data rate for the non-LOS users cannot be guaranteed.

In [6], authors proposed to use passive metallic reflectors to enhance the mmWave signal coverage in the indoor non-LOS

propagation scenario. Various shapes and orientation of reflectors have been examined to achieve the maximal power gain. However, the measurement setup does not reveal the practical 5G NR setting since the mmWave signal generation was taken place in an indoor environment and tested in the closed surroundings.

To the best of our knowledge, the use of LAN cable based relay system for extending the outdoor mmWave coverage to the indoor environment has not been reported in any literature.

B. A2C Scheduler

A2C mapping was defined in [7] as to determine which antenna signals are carried by each sub-carrier of a specific twisted pair of the cable bundle, along with the power allocated to the sub-carrier. Such mapping is necessary to form a signal path for each antenna for both UL and DL transmissions. The MP-A2C scheduler introduced in [7] aims to achieve real-time A2C mapping on a multi-pair LAN cable such that the largest number of antennas can be supported while meeting the quality requirement of the antenna signals.

Fig. 2 demonstrates the basic idea of MP-A2C scheduler on a single twisted pair. We are given the capacity profile in bits per second per Hz (bit/sec/Hz) of the twisted pair that is used to support 50 MHz antenna signals A1–A8 with various capacity demands ranging from 8 bit/sec/Hz to 2 bit/sec/Hz. Straightforward allocation of the 8 antenna signals across the cable spectrum may lead to poor performance as shown in the bottom of Fig. 2, where two antenna signals (A7 and A8) cannot be accommodated due to insufficient cable capacity at the frequency 300–400 MHz. Nonetheless by manipulating the translated frequency and power shaping of each antenna signal, all the 8 antennas signals can be accommodated as shown in the top of Fig. 2.

In the event of multiple twisted pairs, the MP-A2C scheduling problem becomes more complicated by additionally considering the FEXT between the antenna signals of the same frequency while being transmitted along two different twisted pairs of a common cable bundle.

III. PROPOSED MMWAVE ACCESS ARCHITECTURE

As shown in Fig. 1, the proposed mmWoC based network access has each room on each floor to be equipped with an IRU, which is in turn connected to the mmSC via a cable bundle with one or multiple LAN cables. Different from SUDAS [4], mmWave spectrum is used both at front-end (UE → mmSC) and back-end (mmSC → mmBS), whereas the mmWave signals are received at mmSC and transported to each chamber via LAN cable.

Fig. 3 shows the functional diagram of the proposed mmWoC based access network. Distinguished from the conventional mmWave coverage solution, the proposed mmSC hosts a local antenna array (LAA) for outdoor coverage, while the indoor coverage are provisioned through the IRUs that can be located up to 200 m away from the mmSC. Particularly, the IRU is an all-analog indoor device hosting a rectangular antenna array that can be accessed by the indoor 5G users via mmWave transmissions; and it is connected with the mmSC via an inter-

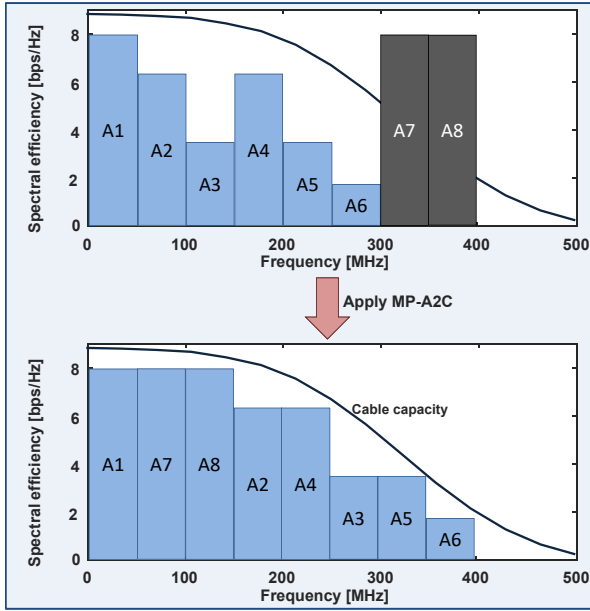


Fig. 2. An example of MP-A2C scheduler operation for 8 antenna signals on a single twisted pair.

mediate device called analog relay unit (ARU), which performs signal amplification, frequency conversion, and interface with the LAN cables. The transportation of multiple mmWave signals over the LAN cables is carried out by a non-configurable air-to-cable (NC-A2C) scheduler that defines which cable sub-carrier is used to carry a specific mmWave signal of each antenna.

A. Functions of ARU

The functional structure of ARU in the proposed mmWoC access architecture is shown in Fig. 4. The ARU is in an IRU located at the roof of the chamber and hosts 4 rectangular antenna arrays (with multiple antennas per array for analog beamforming) and are driven by 4 RF chains; while the mmSc is located 100m away from the IRU that also contains an ARU as the interface for the mmSC to access the cable spectrum with an achievable channel bandwidth f_{\max} of 400 MHz along each twisted pair. The bandwidth allocated to each antenna in the mmWave spectrum is assumed to be 100 MHz (i.e., $\Delta f_{RF} = 100$ MHz), which means each twisted pair may support up to 4 antenna array signals¹. Without loss of generality, the following discussion considers UL of 4 antenna array signals $x_1 - x_4$ transported over a twisted pair TP1, while the DL is likewise.

The ARU at the IRU receives the 4 mmWave signals $x_1 - x_4$ of the carrier frequencies f_{RF} through the 4 antenna arrays, as shown in Fig 4. To avoid interference among the mmWave signals $x_1 - x_4$, analog precoding is considered in this paper where precoding is achieved through phase shifters only [8],[9]. The signals $x_1 - x_4$ are firstly down-converted to intermediate frequencies (IF) denoted as $f_{IF_1}, f_{IF_2}, \dots, f_{IF_4}$, that fall under the achievable channel bandwidth f_{\max} of TP1. The IF signals

¹Note that the mmWave spectrum bandwidth Δf_{RF} in 5G NR ranges from 50 MHz to 400 MHz, however here we consider $\Delta f_{RF} = 100$ MHz just as an example to describe the ARU functionality.

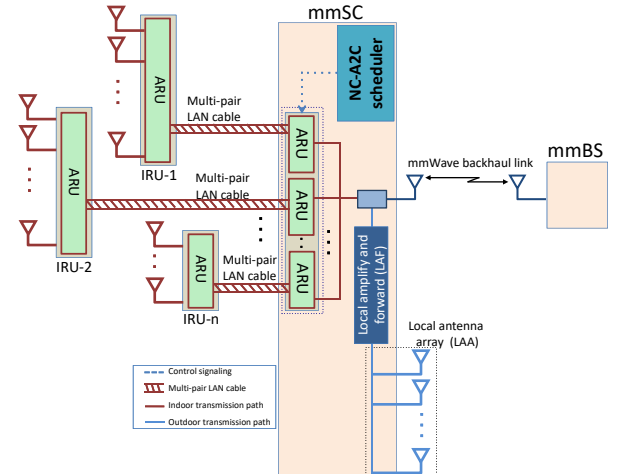


Fig. 3. Functional diagram of the proposed mmWoC based access network architecture for indoor coverage.

$x_1 - x_4$ are further power-shaped with a pre-defined power scaling, which are then frequency-multiplexed to form a single composite signal that can be transmitted over TP1.

This composite signal is received by the ARU of the mmSC and fed to an analog IF band-pass filter bank, where the pass-band of each filter is considered to be 100 MHz and the central IF frequencies for the signals x_1 to x_4 are $f_{IF_1}, f_{IF_2}, \dots, f_{IF_4}$. Then the mmWave signals are restored after undergoing another frequency conversion stage where the IF signals are up-converted to the mmWave spectrum with frequency f_{RF} .

B. NC-A2C Scheduler

Although MP-A2C scheduler defined in [7] can achieve optimal performance, it imposes stringent requirements on the system control and is not feasible in the mmWave scenario. Since the radio channel conditions in mmWave spectrum fluctuate rapidly with time, the scheduling decision has to be made in every time frame that causes significant computation overhead. Further, a scheduling decision should be conveyed timely to the IRU so as to configure the active devices in the IF-to-RF converters along the signal path such as amplifiers, frequency mixers, filters. Hence an active real-time signaling protocol is required between the mmSC and IRU to practically implement the MP-A2C scheduler.

In the proposed mmWoC access architecture, we employ a novel non-configurable A2C (NC-A2C) architecture that is characterized by the fixed mapping between the mmWave RF signals and cable sub-carriers. By taking Fig. 4 as an example, the mmWave signal x_1 received at the first antenna of the IRU is always mapped to the central frequency f_1 of TP1 and goes through the predefined analog processing operations including frequency conversion and power shaping. These analog operations on x_1 is disregard with how x_1 is modulated according to the fluctuating channel.

Clearly, the use of analog processing units that are not dynamically configurable is expected to not only achieve considerable cost reduction, but also avoid the high computational complexity and real-time control signaling effort between the mmSC and

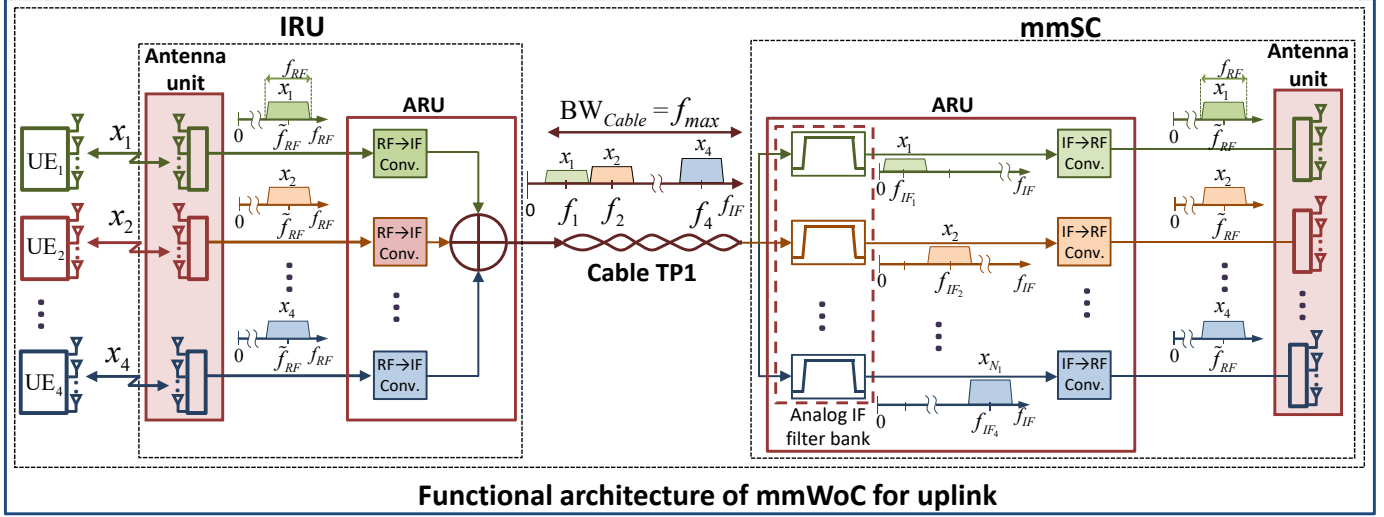


Fig. 4. Functional architecture of ARU at IRU and mmSC for uplink.

IRU. In specific, the NC-A2C has all the analog devices in the ARU to be one-time configured as if all the antenna signals are highest modulated prior to the operation, and these configured parameters are kept constant afterward.

Obviously, NC-A2C gains all the mentioned advantages at the expense that some cable capacity may be wasted when any antenna signal takes a lower modulation. Such a trade-off will be of interest and well investigated in the rest of the paper.

IV. SYSTEM MODEL

Without loss of generality, we take UL transmission to demonstrate the system model of the proposed mmWoC access architecture. The number of total UEs is denoted as $N_{UE} = N_1 + N_2 + N_3 + N_4$, and each UE sends one data stream to IRU by forming an analog beam and corresponds to a single radio signal, where N_i denotes the number of radio signals that can be mapped over twisted pair i . The IRU hosts N_{RF} RF chains with K antennas attached to each RF chain, hence the total number of antennas to serve N_{UE} UEs are $N_U = KN_{RF}$. Here, we have assumed that the number of users that IRU can support is limited by the number of RF chains, i.e., $N_{UE} \leq N_{RF}$. Assuming single data stream from each user and same transmission frequency for all the UEs (i.e., \tilde{f}_{RF}), the transmitted signal from the l th UE to IRU is given by

$$\mathbf{s}_l = \mathbf{f}_{RF,l} d_l, \quad (1)$$

where $\mathbf{f}_{RF,l} \in \mathbb{C}^{K \times 1}$ and $d_l \in \mathbb{C}^{1 \times 1}$ are the transmit analog beamforming vector and data symbol from the l th UE, respectively. The transmit signal power P_l from l th UE is constrained by $\mathbb{E}[|\mathbf{s}_l|^2] \leq P_l$. The received signal $\bar{\mathbf{s}}$ at the IRU is

$$\bar{\mathbf{s}} = \sum_{l=1}^{N_{UE}} [\mathbf{H}_{UE \rightarrow IRU}]_l \mathbf{s}_l + \bar{\mathbf{n}}_a = \sum_{l=1}^{N_{UE}} [\mathbf{H}_{UE \rightarrow IRU}]_l \mathbf{f}_{RF,l} d_l + \bar{\mathbf{n}}_a. \quad (2)$$

Here, $[\mathbf{H}_{UE \rightarrow IRU}]_l \in \mathbb{C}^{N_U \times K}$ is the indoor mmWave channel matrix from the l th UE to IRU, while $\bar{\mathbf{n}}_a \in \mathbb{C}^{N_U \times 1}$ is the additive white Gaussian noise (AWGN) vector with zero mean and

variance σ_a^2 at each antenna of IRU.

Assuming w_k^i is the value of phase shifter of k th antenna in the i th RF chain at IRU, the corresponding receive analog beamforming vector for i th RF chain at IRU can be written as

$$\mathbf{w}^i = [w_1^i, w_2^i, \dots, w_K^i]^T. \quad (3)$$

Hence, the $K \times N_U$ block diagonal analog beamforming matrix at the IRU is comprised by K antennas arrays as

$$\mathbf{W} = blkdiag[\mathbf{w}_1^T, \mathbf{w}_2^T, \dots, \mathbf{w}_{N_U}^T]. \quad (4)$$

The signal $\bar{\mathbf{s}}$ at the IRU in Fig. 5 after the receiver analog beamforming matrix is

$$\begin{aligned} \bar{\mathbf{s}} &= \mathbf{W} \sum_{l=1}^{N_{UE}} [\mathbf{H}_{UE \rightarrow IRU}]_l \mathbf{s}_l + \mathbf{W} \bar{\mathbf{n}}_a \\ &= \sum_{l=1}^{N_{UE}} \mathbf{W} [\mathbf{H}_{UE \rightarrow IRU}]_l \mathbf{f}_{RF,l} d_l + \mathbf{n}_a \\ &= \sum_{l=1}^{N_{UE}} \mathbf{h}_l^a d_l + \mathbf{n}_a \\ &= [\mathbf{h}_1^a \quad \mathbf{h}_2^a \quad \dots \quad \mathbf{h}_{N_{UE}}^a] \begin{bmatrix} d_1 \\ d_2 \\ \vdots \\ d_{N_{UE}} \end{bmatrix} + \mathbf{n}_a, \end{aligned} \quad (5)$$

here $\mathbf{n}_a = \mathbf{W} \bar{\mathbf{n}}_a$ and $\mathbf{h}_l^a = \mathbf{W} [\mathbf{H}_{UE \rightarrow IRU}]_l \mathbf{f}_{RF,l}$ is the effective channel vector between the l th UE and IRU. In this paper, we have assumed that analog beamforming is achieved only through phase variation, therefore all the values of transmit and receive analog beamforming matrices can be written as $e^{j\theta}$ where $\theta \in [0, 2\pi]$ is the phase of the phase shifters.

Let each cable sub-carrier be equally spaced with bandwidth Δf_{cable} , where a number of $N_F = \lfloor \text{BW}_C / \Delta f_{cable} \rfloor$

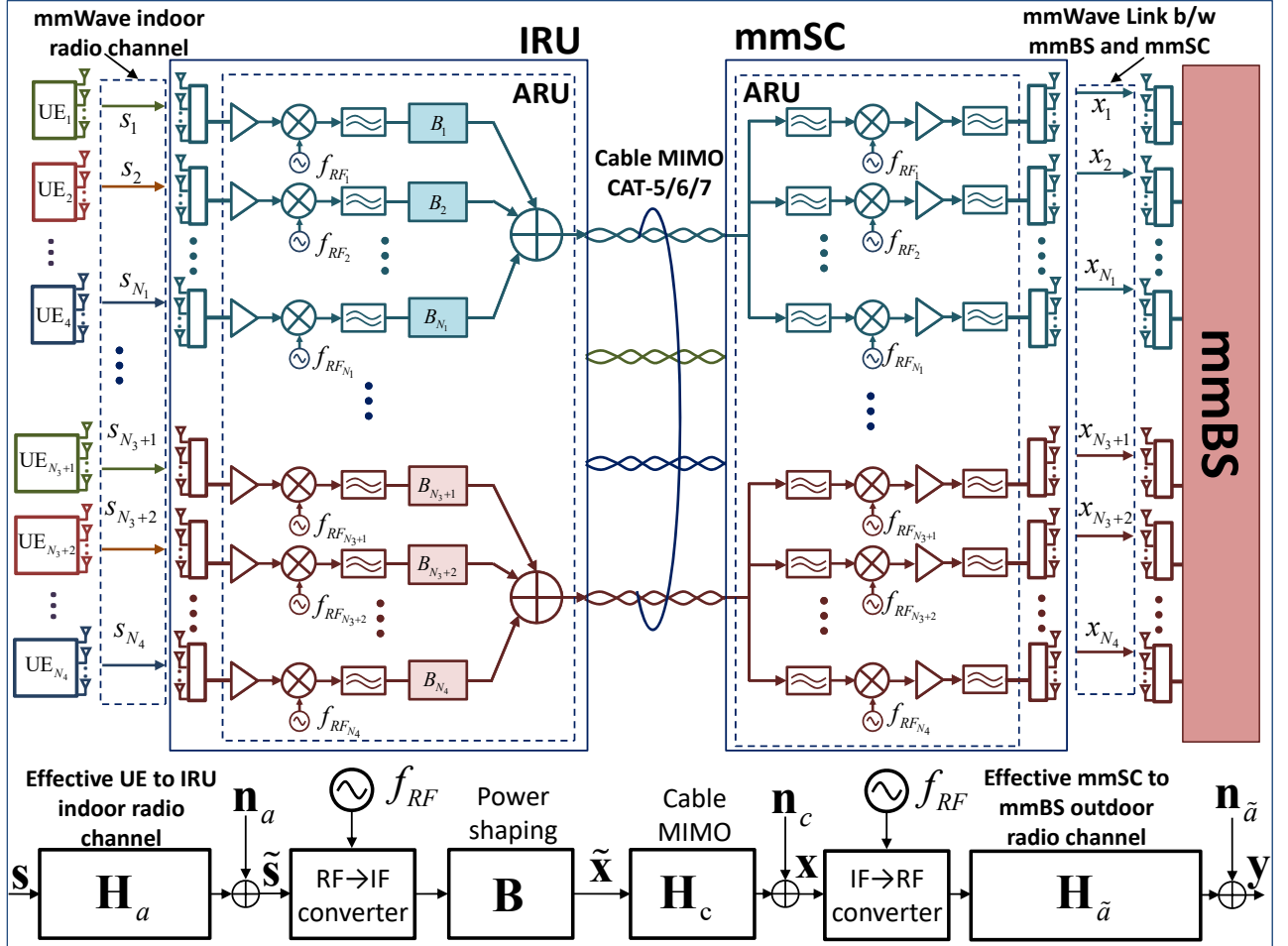


Fig. 5. System model for uplink transmission via mmWoC architecture.

sub-carriers per cable are in place. Thus, the cumulative cable bandwidth (summation of achievable bandwidth over each twisted pair) is BW_C . Let the coherence bandwidth over a single mmWave radio channel and the number of radio sub-channels be denoted as Δf_{air} and $N_R = \lfloor BW_{5G} / \Delta f_{air} \rfloor$, respectively, where BW_{5G} is the available mmWave spectrum bandwidth.

To launch the antenna signals on the cable sub-carriers, the RF→IF frequency converter corresponding to each antenna at the IRU should be well tuned based on the NC-A2C scheduling decision. Let the low-noise amplifiers (LNA) and mixers in the IRU be tuned at the frequency $f_{RF} \in \{f_{RF_1}, \dots, f_{RF_{N_1}}, f_{RF_{N_1+1}}, \dots, f_{RF_{N_2}}, \dots, f_{RF_{N_4}}\}$, so as to down convert each UE signal to different IF such as $f_{IF} \in \{f_{IF_1}, \dots, f_{IF_{N_1}}, f_{IF_{N_1+1}}, \dots, f_{IF_{N_2}}, \dots, f_{IF_{N_4}}\}$, while the central frequency of bandpass filters are accordingly set to f_{IF} as well. All the tunable components in the IRU are configured prior to the installation and once configured, and the antenna mmWave signals are pre-configured to map to fixed cable sub-channels of a given twisted pair.

The RF→IF converters in Fig. 5 perform down-conversion on the received RF signals $\tilde{\mathbf{s}}$, which are then power shaped according to a block diagonal matrix \mathbf{B} . This power shaping matrix \mathbf{B} should be designed so as to minimize the far end crosstalk

(FEXT) among the twisted pairs. Let the received IF composite signal vector at the mmSC be denoted as $\mathbf{x} \in \mathbb{C}^{N_{UE}}$, which can be further expressed as:

$$\mathbf{x} = \mathbf{H}_c \mathbf{B} \tilde{\mathbf{s}} + \mathbf{n}_c, \quad (6)$$

where $\mathbf{H}_c \in \mathbb{C}^{T_C N_C N_F \times T_C N_C N_F}$ is the frequency-dependent cable channel between the IRU and mmSC, and $\mathbf{n}_c \sim \mathcal{CN}(\mathbf{0}, \sigma_C^2 \mathbf{I})$ is the AWGN with power spectral density (PSD) σ_C^2 . The cable binder contains T_C LAN cables with N_C twisted pairs each. The orthogonal sub-carriers in a cable binder can be mathematically modeled as a block-diagonal matrix with N_F diagonal elements

$$\mathbf{H}_c = \text{diag}[\mathbf{H}_{c,1}, \mathbf{H}_{c,2}, \dots, \mathbf{H}_{c,N_F}], \quad (7)$$

where $\mathbf{H}_{c,k}$ represents $T_C N_C \times T_C N_C$ MIMO cable channels across the k th sub-carrier. Here the diagonal elements of $\mathbf{H}_{c,k}$ shows the direct link between the IRU and mmSC, while the off diagonal terms represent the FEXT coefficients among cable binder pairs across the k th sub-carrier [10], [11]. The capacity of a cable binder depends on the number of LAN cables in a binder (i.e., T_C), LAN cable type (CAT5/6/7), cable binder length and achievable transmission bandwidth over each twisted pair. The measurements results for 100 m, 125 m, 150 m, 175 m, and 200 m CAT-5, CAT-6, and CAT-7 cables can be found in [10].

At the mmSC, the IF→RF converters are tuned such that the RF frequencies of the oscillators are set to $f_{RF} \in \{f_{RF_1}, \dots, f_{RF_{N_1}}, f_{RF_{N_1+1}}, \dots, f_{RF_{N_2}}, \dots, f_{RF_{N_4}}\}$, so as to achieve all the signals with same mmWave frequency as \tilde{f}_{RF} .

The identical analog beamforming is applied between mmSC → mmBS as in UE → IRU, and the received signals after beamforming at the mmBS can be expressed as:

$$\tilde{\mathbf{y}} = \mathbf{H}_{\tilde{a}} \mathbf{x} + \mathbf{n}_{\tilde{a}}. \quad (8)$$

Here, $\mathbf{H}_{\tilde{a}} \in \mathbb{C}^{N_{UE} \times N_{UE}}$ is the effective channel matrix between the mmSC and mmBS after analog beamforming, where its diagonal components represent the channel gains between the RF chains of the mmSC and mmBS. All the signals are scaled at the mmSC such that the transmit power is compliant with the ITU standard defined for inter-site distance between the mmSC and mmBS. The AWGN $\mathbf{n}_{\tilde{a}} \sim \mathcal{CN}(\mathbf{0}, \sigma_{\tilde{a}}^2 \mathbf{I})$ with flat PSD (i.e., $\sigma_{\tilde{a}}^2$) is assumed at the antenna array of the mmBS.

A. mmWave Radio Channel Model

Two separate mmWave links are defined in the proposed mm-WoC architecture. One is the outdoor LOS mmWave radio link between the mmBS and mmSC that forms back-end (BE) access to the core network and represented by $\mathbf{H}_{\tilde{a}}$ in (8). The other is the indoor LOS mmWave radio link \mathbf{H}_a in 5.

The sparse geometric channel model [12] is used in this paper for both indoor and outdoor LOS mmWave Radio channels. This is a widely used mmWave channel model that describes the radio channel in terms of physical rays between the transmitter and receiver, hence also called ray-based channel model. The general channel vector between the transmitter and antenna u of the receiver is

$$\mathbf{h}_u = \sum_{p=1}^L \beta_{u,p} \mathbf{a}^H(\theta_{u,p}) \in \mathbb{C}^{N_u \times 1}, \quad (9)$$

such that $\beta_{u,p}$ is the complex path gain from the user to the u th antenna along the p th path, where L is the total number of paths from the transmitter to the antenna element u of the receiver. The angle of arrival (AoA) at the u th antenna for each path p is $\theta_{u,p}$, which is assumed to be uniformly distributed $\theta_{u,p} \sim \mathcal{U}(0, 2\pi)$. The received steering vector $\mathbf{a}(\theta_{u,p})$ is $\mathbf{a}(\theta_{u,p}) = [1 \ e^{j\pi \sin(\theta_{u,p})} \ \dots \ e^{j\pi(N_u-1) \sin(\theta_{u,p})}]^T$. The propagation constant $\beta_{u,p}$ in (9) is based on the geometric path loss model given by $\beta_{u,p}$ [dB] = $\alpha(f_c) + \gamma 10 \log_{10}(d_{3D}) + \xi$, where $\alpha(f_c)$ is the frequency dependant path loss constant, γ is the path loss exponent, d_{3D} is the 3D Euclidean distance between the transmitter and receiver, and ξ is the log-normal shadow fading coefficient.

The 28 GHz band has been used in this paper for outdoor mmWave link between the mmSC and mmBS. The motivations behind this choice are; 1) there is a vast amount of under-utilized licensed mmWave bands around 28 GHz that can support 500 m inter-site distance, 2) a multi-path environment still exists as compared to higher frequency bands such as 60 GHz, and 3) the 3GPP LTE functionalities can be reused by allowing 28 GHz band as a backhaul link since the LTE physical layer was originally designed to work up to 40 GHz for SC backhaul links.

The 5GCM urban macro LOS (UMa-LOS) model [12] has been considered to realize the outdoor mmWave radio link between the mmBS and mmSC, hence the path loss coefficient $\alpha(f_c)$ is expressed as:

$$\alpha_{mmSC \rightarrow mmBS}(f_c) = 32.4 + 20 \log_{10}(f_c), \quad (10)$$

where $\gamma_{mmSC \rightarrow mmBS} = 21$. The indoor mmWave radio channel between the UEs and IRU is modeled in this paper using the mmMAGIC model, which is applicable for an indoor office environment for the mmWave spectrum ranging from 6 GHz to 100 GHz. The path loss for the indoor LOS and NLOS channels are expressed as

$$\alpha_{UEs \rightarrow IRU}^{(LOS)}(f_c) = 32.4 + 20 \log_{10}(f_c), \quad (11)$$

$$\alpha_{UEs \rightarrow IRU}^{(NLOS)}(f_c) = \max(\alpha_{UEs \rightarrow IRU}^{(LOS)}(f_c), \alpha_{UEs \rightarrow IRU}^{(NLOS)}(f_c)), \quad (12)$$

$$\alpha_{UEs \rightarrow IRU}^{(NLOS)}(f_c) = 17.3 + 24.9 \log_{10}(f_c). \quad (13)$$

The $\gamma_{UEs \rightarrow IRU} = 17.3$ for both LOS and NLOS scatters. The mmWave radio channels for $mmSC \rightarrow mmBS$ and $UEs \rightarrow IRU$ in (8) and (5) become:

$$\mathbf{H}_{\tilde{a}} = [\mathbf{h}_1, \mathbf{h}_2, \dots, \mathbf{h}_u, \dots, \mathbf{h}_{N_U}]^T \quad (14)$$

$$\mathbf{H}_a = [\mathbf{h}_1, \mathbf{h}_2, \dots, \mathbf{h}_u, \dots, \mathbf{h}_{N_U}]^T. \quad (15)$$

Due to effective analog beamforming, all the indoor and outdoor signals are assumed to be spatial multiplexed without effecting the channel gains, hence the effective channels $\mathbf{H}_{\tilde{a}}$ and \mathbf{H}_a become diagonal channels in which the channel gain between each transmitter and receiver antenna pair lies on the main diagonal.

B. Transmission Rates over mmWave Spectrum

The transmission model used in this paper is based on 5G NR specification, where μ as $\Delta f_{SCS} = 2^\mu \cdot 15$ kHz define the sub-carrier spacing (SCS). The parameter μ ranges from 2 to 4 for various deployment scenarios, i.e., indoor, outdoor and small cell [13]. Each physical resource block (PRB) contains N_{sc}^{RB} sub-carriers and the radio channel is assumed to be flat across all the sub-carriers in a PRB. The sub-channel bandwidth for one PRB can be computed as $\Delta f = N_{sc}^{RB} \Delta f_{SCS} = N_{sc}^{RB} 2^\mu \cdot 15$ kHz.

The achievable SINR of the mmWave effective physical link can be closely approximated by the path loss model of the considered scenario. The SINR $[\text{SINR}_{5G}]_{u,r}$, $\forall u \in \{1, \dots, N_{UE}\}$ and $\forall r \in \{1, \dots, N_R\}$ for sub-channel r corresponds to multiple Δf resource blocks over a single OFDM symbol duration in 5G and can be computed as

$$[\text{SINR}_{5G}]_{u,r} = \frac{PL_{u,u}^{-1} P_{u,u}}{\sum_{l \neq u} PL_{u,l}^{-1} P_{u,l} + \Delta f N_0}, \quad (16)$$

where $P_{u,l}$ is the signal power from transmitter l , $\Delta f N_0$ is the thermal noise, and $PL_{u,l}$ represents the linear path loss between transmitter l and receiver u , which can be further expressed as

$$PL_{u,l} = \alpha(f_c) + \gamma 10 \log_{10}(d_{3D}). \quad (17)$$

Since all the channels between transmitter and receiver in mmWave spectrum are considered to be spatial multiplexed, the interference in (16) can be ignored and the SNR at the receiver would be

$$[\text{SNR}_{5G}]_{u,r} = \frac{PL_{u,u}^{-1}P_{u,u}}{\Delta f N_0}. \quad (18)$$

Also BW_{5G} is considered to be flat across Δf , thus, the corresponding bit rates ($\mathbf{R}_{5G} \in \mathbb{R}^{N_{UE} \times N_R}$) are assumed to be quasi-constant within a sub-channel Δf . The bit rate on each sub-channel Δf over a single OFDM symbol duration, i.e., $[\mathbf{R}_{5G}]_{u,r}$, can be computed as:

$$[\mathbf{R}_{5G}]_{u,r} = \lfloor \log_2 (1 + [\text{SNR}_{5G}]_{u,r}) \rfloor. \quad (19)$$

V. A2C PROBLEM FORMULATIONS

A. NC-A2C Problem: P_{NC-A2C}

We formulate the NC-A2C optimization problem with an objective to maximize the number of cable sub-carriers with the capacity of 8 bits/sec/Hz. The following optimization variables are required for the NC-A2C problem:

- $x_{n,k}$ is an assignment variable, which is 1 if sub-carrier $k \in \{1, \dots, N_{SC}\}$ can achieve a spectral efficiency of 8 bits/sec/Hz and 0 otherwise.
- $P_{n,k}$ is for allocating power to the k th sub-carrier of the n th cable pair.
- $I_{n,k}$ is for computing interference on the k th sub-carrier of the n th cable pair.

Given the cable channel matrix (i.e., \mathbf{H}_c with $h_n^{n,k}$ as the direct channel gains and $h_n^{n',k}$ as the off-diagonal channel gains), the NC-A2C optimization problem can be defined as follows:

$$P_{NC-A2C} : \underset{\{x_{n,k}\}, \{P_{n,k}\}, \{I_{n,k}\}}{\text{maximize}} \sum_{n=1}^{T_C N_C} \sum_{k=1}^{N_{SC}} x_{n,k}$$

subject to:

$$x_{n,k} \in \{0, 1\}, \quad \forall n, \forall k \quad (20a)$$

$$x_{n,k} \geq x_{n,k+1}, \quad \forall n, \forall k \quad (20b)$$

$$0 \leq P_{n,k} \leq x_{n,k} P_{\max}, \quad \forall n, \forall k \quad (20c)$$

$$\sum_{k=1}^{N_{SC}} P_{n,k} \leq P_T, \quad \forall n \quad (20d)$$

$$P_{n,k} |h_n^{n,k}|^2 \geq \beta(I_{n,k} + \sigma_C^2) - (1 - x_{n,k})M, \forall n, \forall k \quad (20e)$$

$$I_{n,k} = \sum_{n'=1, n' \neq n}^{T_C N_C} P_{n',k} |h_n^{n',k}|^2, \quad \forall n, \forall k \quad (20f)$$

where, $n \in \{1, \dots, T_C N_C\}$, $k \in \{1, \dots, N_F\}$, and M is a very large number. β is the SINR threshold for achieving a spectral efficiency of 8 bits/sec/Hz and σ_C^2 is the noise power per sub-carrier of the cable. The sum of the power of all sub-carriers for each twisted pair is constrained by the total transmit power (i.e., P_T), leading to the fact that the maximum power of the transmitted signals over the cable is also constrained by the maximum power spectral density (i.e., $P_{n,k} \leq P_{\max}$).

The constraints (20b) ensure that the spectral efficiency is monotonically decreasing with the increase of frequency. The constraints (20c), and (20d) ensure that the transmit power over each cable sub-carrier is not higher than the specified values. The constraints (20e) and (20f) are for computing appropriate power and interference, respectively. Note that if $x_{n,k} = 0$, the inequality (20e) is true for all values of $P_{n,k}$ and $I_{n,k}$ because the right hand side has a very large negative value. On the other hand, if $x_{n,k} = 1$, the inequality states that $P_{n,k} |h_n^{n,k}|^2 \geq \beta(I_{n,k} + \sigma_C^2)$ and this is exactly desired.

Note that different from the MP-A2C optimization formulation in [7], the NC-A2C scheduler is designed to maximize the copper channel bandwidth for spectral efficiency of 8 bits/sec/Hz.

B. MP-A2C Problem: P_{MP-A2C}

MP-A2C attempts to maximize the number of cable sub-carriers with a capacity of either 2, 4, 6, or 8 bits/sec/Hz, depending on the input antenna signal modulation schemes. In addition to all the variables defined for the NC-A2C formulation, the following additional optimization variables are required in the proposed MP-A2C formulation:

- $x_{n,k}^b$ is an assignment variable, which is 1 if sub-carrier $k \in \{1, \dots, N_{SC}\}$ can achieve a spectral efficiency of b bits/sec/Hz and is 0 otherwise.

Given the cable channel matrix (i.e., \mathbf{H}_c with $h_n^{n,k}$ as the direct channel gains and $h_n^{n',k}$ as the off-diagonal channel gains), the MP-A2C optimization problem is defined as follows:

$$P_{MP-A2C} : \underset{\{x_{n,k}^b\}, \{P_{n,k}\}, \{I_{n,k}\}}{\text{maximize}} \sum_{\forall b} \sum_{n=1}^{T_C N_C} \sum_{k=1}^{N_{SC}} b x_{n,k}^b$$

subject to:

$$x_{n,k}^b \in \{0, 1\}, \quad \forall b, \forall n, \forall k \quad (21a)$$

$$\sum_{\forall b} x_{n,k}^b \leq 1, \quad \forall n, \forall k \quad (21b)$$

$$\sum_{\forall b} b x_{n,k}^b \geq \sum_{\forall b} b x_{n,k+1}^b, \quad \forall n, \forall k \quad (21c)$$

$$0 \leq P_{n,k} \leq (\sum_{\forall b} x_{n,k}^b) P_{\max}, \quad \forall n, \forall k \quad (21d)$$

$$\sum_{k=1}^{N_{SC}} P_{n,k} \leq P_T, \quad \forall n \quad (21e)$$

$$P_{n,k} |h_n^{n,k}|^2 \geq \beta_b (I_{n,k} + \sigma_C^2) - (1 - x_{n,k}^b) M, \forall b, \forall n, \forall k \quad (21f)$$

$$I_{n,k} = \sum_{n'=1, n' \neq n}^{T_C N_C} P_{n',k} |h_n^{n',k}|^2, \quad \forall n, \forall k \quad (21g)$$

where, $b \in \{2, 4, 6, 8\}$, $n \in \{1, \dots, N_C\}$, $k \in \{1, \dots, N_F\}$, M is a very large number, and β_b is the SINR thresh-hold for

Table 1. 5G NR physical layer parameters for space frequency resource allocation.

5G user BW (BW_{5G})	50 MHz
Duplexing scheme	TDD
Modulation scheme	BPSK, QPSK, 16-QAM 64-QAM, 256-QAM
Sub-carrier spacing parameter (μ)	3 (for mmWave spectrum)
Sub-carrier spacing (Δf_{SCS})	120 kHz
No. of sub-carrier per PRB (N_{sc}^{RB})	12
Sub-channel bandwidth (Δf)	$N_{sc}^{RB} \Delta f_{SCS} = 1.44$ MHz
OFDM symbols/sub-frame ($N_{symb}^{subframe}$)	8×14
Sub-frame duration ($T^{subframe}$)	1 ms
Path loss constant ($\alpha(f_c)$)	(10) for outdoor (11), (12), (13) for indoor
Path loss exponent (γ)	21 for outdoor 17.3 for indoor
Shadow fading coefficient (ξ)	$\mathcal{N}(0, \sigma^2)$ with $\sigma = 4$ dB for outdoor $\sigma = 3$ dB for indoor (LOS) $\sigma = 8.03$ dB for indoor (NLOS)

achieving a spectral efficiency of b bits/sec/Hz. The constraints (21b) ensure that only one bit rate is assigned over each cable sub-carrier, whereas the constraints (21c) ensure that the spectral efficiency is monotonically decreasing with the increase in frequency.

VI. PERFORMANCE EVALUATION

The performance of NC-A2C in the proposed mmWoC access architecture is evaluated and compared with the case of MP-A2C [7] that is considered the optimal scenario of cable spectrum resource usage in presence of fluctuating air channels. We are interested in observing the compromise achieved by NC-A2C in terms of total throughput and the number of antennas at the IRU.

A. Physical Layer Parameters

The IRU is assumed to be installed at the center of the roof of a space with 100 m radius. The 28 GHz mmWave band is used between the mmSC and mmBS as the outdoor backhaul inter-site channel, whereas the channel gains are modeled using

Table 2. LAN cable physical layer parameters.

Multi-pair cables	CAT-5 and CAT-7
Number of twisted pairs/ cable ($T_C N_C$)	4
Cable lengths	100 m, 150 m, and 200 m
Cable bandwidth (BW_{Cable})	500 MHz
Sub-carrier bandwidth (Δf)	1.44 MHz
Sum power per line (P_T)	7.5 dBm
Maximum transmit PSD mask (P_{max})	-70 dBm/Hz
Cable noise PSD (σ_C)	-140 dBm/Hz

(9), (10), and (15). The indoor mmWave spectrum is assumed to be 40 GHz, where (9), (11), (12), (13), and (14) are used for channel modeling. Table 1 shows the 5G NR physical layer and transmission parameters considered in this simulation. Time division duplex (TDD) is employed as the duplexing scheme, while the modulation schemes defined under LTE are taken, i.e., BPSK, QPSK, 16-QAM, 64-QAM, and 256-QAM, which corresponds to 1, 2, 4, 6, and 8 bits/sec/Hz of required capacity efficiency. The 5G NR numerology for mmWave coverage is 3 (i.e., $\mu=3$), which results in a sub-carrier spacing Δf_{SCS} equal to 120 kHz ($\Delta f_{SCS} = 2^\mu \cdot 15$ kHz). Thus, the channel bandwidth for one physical resource block (PRB) ($N_{sc}^{RB} \Delta f_{SCS}$) is 1.44 MHz since one PRB contains 12 sub-carriers in the frequency domain. For 5G NR, 8 slots² is contained in each sub-frame with 1 ms duration (i.e., $T^{subframe}= 1$ ms), hence the OFDM symbols per sub-frame is 112.

To the best of our survey, there has no any explicit measurement result on cable binders reported in the literature. Thus the study firstly conducted a set of experiments to gain its basic channel characteristics, specifically the H matrix of the cable binder that is required in the NC-A2C scheduling problem formulation. The experiment settings and results are given in the Appendix.

Table 2 summarizes the physical layer parameters of the copper cable bundle employed in the section. The maximum usable channel spectrum over a LAN cable is obtained by limiting the transmission power of a sub-carrier and sum power per line to -70 dBm/Hz and 7.5 dBm, respectively. In NC-A2C, we require all the sub-carriers to be with a spectral efficiency of 8 bits/sec/Hz which corresponds to the highest modulation scheme for 5G NR, i.e., 256-QAM, while the spectral efficiency in MP-A2C can be adaptive to the air channel condition in the spectrum of 500 MHz.

The two problems P_{NC-A2C} and P_{MP-A2C} are solved by using a commercially available linear integer programming solver (SCIP [14]), where the modulation schemes taken by the input antenna signals are randomly picked up among 1, 2, 4, 6, and 8 bits/sec/Hz.

As shown in Figs. 6 and 7, the proposed NC-A2C achieves lower throughput and supports smaller numbers of antennas than

²One slot contains 14 OFDM symbols with normal cyclic prefix (CP).

Table 3. The number of 50 MHz cable sub-channels with spectral efficiency of 8 bits/sec/Hz.

Scheduler type	Cable type	Cable length		
		100 m	150 m	200 m
NC-A2C	CAT-5	21	11	7
	CAT-7	26	16	11
MP-A2C	CAT-5	14	10	6
	CAT-7	20	14	10

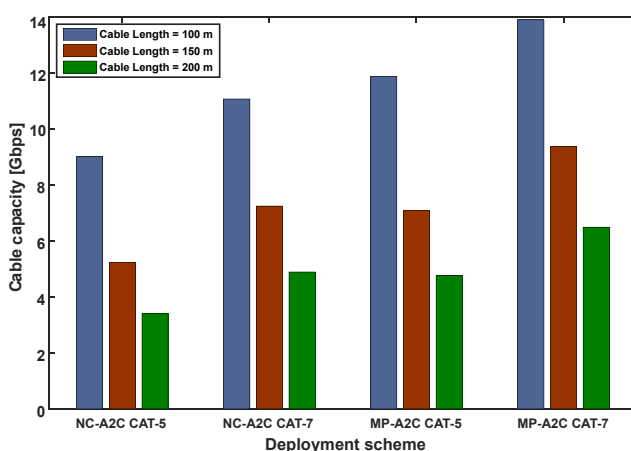


Fig. 6. Cable capacity (in Gbps) achieved by all the considered scenarios.

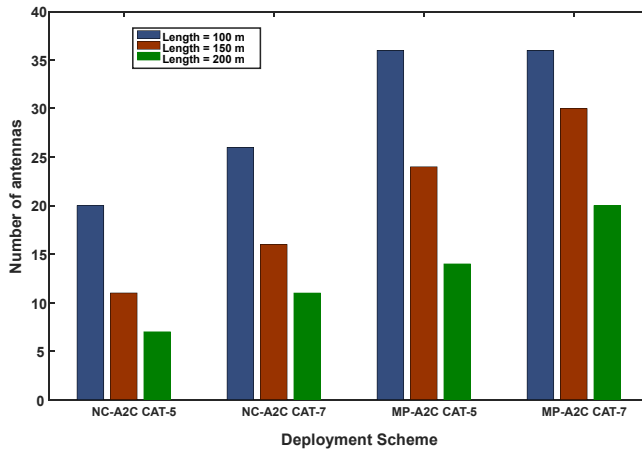


Fig. 7. The number of antennas supported in all the considered scenarios.

that by MP-A2C in all the considered scenarios. This is driven by the fact that NC-A2C ensures the highest possible spectral efficiency (i.e., 8 bits/sec/Hz) for every cable sub-carrier, no matter whether necessary or not. Further, we see that with longer distance of the cable, the cable capacity and number of antennas are both significantly reduced; and the use of CAT-7 cables provides over 20% performance boost against the case of using CAT-5 cables. Fig. 8 shows the total power allocated to the

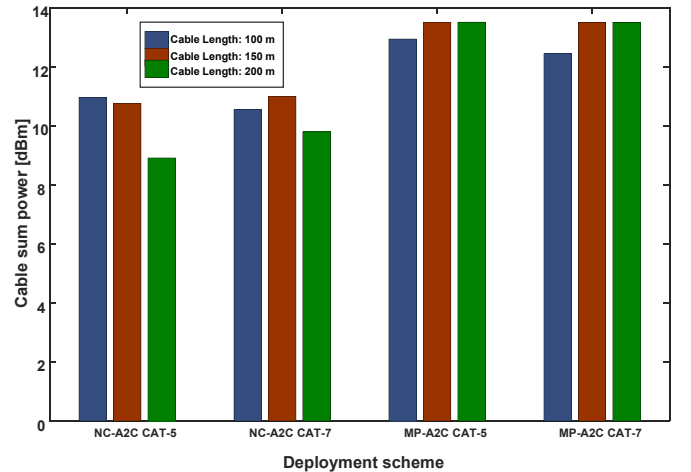


Fig. 8. The sum power (in dBm) on the cable in all the considered scenarios.

cable (containing 4 twisted pairs with 7.5 dBm sum power per line) in each considered scenario, where we see that the cables with MP-A2C are always allocated with larger total power. This is due to the possible accommodation of antenna signals with capacity efficiency less than 8 bits/sec/Hz.

Table 3 shows the experiment result in terms of the achievable number of sub-carriers of 8 bits/sec/Hz over the cable, where MP-A2C is naively used in a non-configurable IRU thus only 8 bits/sec/Hz sub-carriers are usable. NC-A2C is seen to yield significantly more such sub-carriers than that by MP-A2C, thanks to the fact that NC-A2C concentrates its power allocation to the low-frequency sub-carriers given the total power budget.

VII. CONCLUSIVE REMARKS

This paper investigated a novel mmWave access architecture, called mmWoC, for achieving effective mmWave indoor coverage. The proposed mmWoC architecture is characterized as an all-analog relay based solution where an outdoor mmBS is connected to an mmSC at the building roof top via an mmWave link, and the mmSC is further connected to an indoor IRU of a massive antenna array via a multi-pair LAN cable that provisions mmWave access to the indoor UEs. A novel radio resource mapping scheme was defined, called NC-A2C scheduler, which determines how the mmWave antenna signals are mapped to the sub-carriers of the LAN cable along with their power allocation. It is demonstrated that the NC-A2C can achieve numerous advantages over its counterpart (i.e., MP-A2C) in the aspect of control and hardware complexity at the expense of compromised total throughput, which can well incorporate with the proposed mmWoC architecture for real implementation.

APPENDIX CABLE BUNDLE MEASUREMENT

In the multi-pair LAN cable measurement, we considered a cable binder of 2 LAN cables with 4 twisted pairs in each cable and 50 m in length, where both inter (between the two LAN cables) and intra (within a single LAN cable) cable crosstalks are in place, as shown in Fig. 9. The simulation frequency range is set up to $BW_C = 1$ GHz. The inter and intra coupling of

the cable binder is denoted by $Coupling(ji)$, where " i " and " j " represents the disturber and victim cable, respectively, and the coupling could be due to far end crosstalk (FEXT) or near end crosstalk (NEXT). For example, FEXT(12) shows the intercable FEXT on cable 1 to cable 2.

To properly setup the measurement environment, following devices and equipment are used:

1. Agilent 2/4 port PNA-X network analyzer (PNA) N5242A: Measure S-parameters to characterize any two-port networks such as amplifiers and filters.
2. 2 port calibration kit NA-4691-60008: Remove the effects of systematic errors from the measurements.
3. High frequency Balun transformer NH16447: Transform signals between the coaxial cable (that connects to NA ports) and twisted pair.

In our measurement setup, IL is measured between the opposite ends of a single twisted pair (TP) in a cable binder contains multiple TPs. For example, to measure the IL of TP1, one end of TP1 is connected to port 1 while its opposite end is connected to port 4 at NA. The IL between two ends of a twisted pair is measured by S-parameter S_{41} on PNA. To measure FEXT at TP2 when signal is transmitted from TP, the TP1 and TP2 are connected to port 1 and port 4 respectively. The FEXT between pair 1 and pair 2 is measured by S-parameter S_{41} on PNA. While measuring IL and FEXT, all the ends of remaining TPs are properly terminated using 50 SMA resistors.

The measurement results for the insertion loss (IL) versus FEXT are shown in Fig. 10, where IL is reduced to -40 dB when the signal frequency reaches 1 GHz, while the FEXT is approximately the same. With these results, it can be easily proved that the achievable capacity for 50 m cable binder is 60 Gbps over 1 GHz frequency spectrum.

REFERENCES

- [1] 3GPP, "5G NR; Base station (BS) radio transmission and reception," 3rd Generation Partnership Project (3GPP), Technical Specification (TS) 38.104, 07 2018, version 15.2.0.
- [2] C. Perfecto, J. Del Ser, and M. Bennis, "Millimeter-wave v2v communications: Distributed association and beam alignment," *IEEE J. Sel. Areas Commun.*, vol. 35, no. 9, pp. 2148–2162, Sept. 2017.
- [3] L. D. Heyn and et al., "Cost Model - Country analysis report (CAR) for Germany," FTTH Council Europe, Technical Report (TR), 08 2013, version 1.
- [4] M. Goodarzi, A. Krishnamoorthy, R. Schober, and M. Breiling, "Resource allocation for outdoor-to-indoor amplify-and-forward sudas with independent relay processing," in *Proc. SCC*, Feb. 2019.
- [5] S. Wu, R. Atat, N. Mastronarde, and L. Liu, "Improving the coverage and spectral efficiency of millimeter-wave cellular networks using device-to-device relays," *IEEE Trans. Commun.*, vol. 66, no. 5, pp. 2251–2265, May 2018.
- [6] W. A. G. Khawaja et al., "Effect of passive reflectors for enhancing coverage of 28 ghz mmwave systems in an outdoor setting," in *Proc. IEEE RWS*, Jan. 2019.
- [7] S. H. R. Naqvi, P. H. Ho, and S. Jabeen, "A novel distributed antenna access architecture for 5g indoor service provisioning," *IEEE J. Sel. Areas Commun.*, vol. 36, no. 11, pp. 2518–2527, Nov. 2018.
- [8] O. El Ayach, S. Rajagopal, S. Abu-Surra, Z. Pi, and R. W. Heath, "Spatially sparse precoding in millimeter wave mimo systems," *IEEE Trans. Wireless Commun.*, vol. 13, no. 3, pp. 1499–1513, Mar. 2014.
- [9] A. Alkhateeb, O. El Ayach, G. Leus, and R. W. Heath, "Channel estimation and hybrid precoding for millimeter wave cellular systems," *IEEE J. Sel. Topics Signal Process.*, vol. 8, no. 5, pp. 831–846, Oct. 2014.
- [10] S. H. R. Naqvi, A. Matera, L. Combi, and U. Spagnolini, "On the transport capability of lan cables in all-analog mimo-roc fronthaul," in *Proc. IEEE WCNC*, Mar. 2017.
- [11] A. Matera, L. Combi, S. H. R. Naqvi, and U. Spagnolini, "Space-frequency to space-frequency for mimo radio over copper," in *Proc. IEEE ICC*, July 2017.
- [12] ETSI, "LTE;5G; Study on channel model for frequency spectrum above 6 GHz," 3rd Generation Partnership Project (3GPP), Technical Report (TR) 38.900, 06 2017, version 14.2.0.
- [13] 3GPP, "5G; NR; Physical Channels and Modulation," 3rd Generation Partnership Project (3GPP), Technical Specification (TS) 38.211, 10 2018, version 15.3.0.
- [14] T. Achterberg, "Scip: Solving constraint integer programs," *Mathematical Programming Computation*, vol. 1, no. 1, pp. 1–41, 2009.



Syed Hassan Raza Naqvi received the B.S. degree in Electronics Engg. from SSUET Pakistan, the M.S. (Electrical Engg.) from Linkoping University, Sweden, and the Ph.D. (IT - specialization in Telecommunication) from Politecnico di Milano, Italy. He is currently Post Doctorate Fellow at Department of Electrical and Computer Engineering, University of Waterloo Canada. He has several years of teaching, research and industrial experience. His research interests include interference mitigation in modern wired and wireless technology, channel estimation and equalization, optimize design and implementation of LTE over cable based front hauling, Massive multi-user MIMO, VLSI and FPGA implementation of modern wired and wireless standards.



Pin Han Ho received his Ph.D. degree from Queens University at 2002. He is now a Full Professor in the department of Electrical and Computer Engineering, University of Waterloo, Canada. Pin-Han Ho is the Author/Co-author of more than 350 refereed technical papers, several book chapters, and two books on optical networking and survivability. His current research interests cover a wide range of topics in broadband wired and wireless communication networks. He is the recipient of Distinguished Research Excellent Award in the ECE department of UoW, Early Researcher Award in 2005, the Best Paper Award in SPECTS'02, ICC'05, and ICC'07, and the outstanding Paper Award in HPSR02.



Limei Peng is an Assistant Professor in the School of Computer and Engineering, Kyungpook National University, South Korea, since 2018. She has been an Assistant Professor in the Department of Industrial Engineering, Ajou University, South Korea, from 2014 to 2018. She has Authored/Co-authored for more than 90 research papers in the leading journals and conferences. Her research interests include the Cloud computing, Edge computing, data communications, optical communication networks and protocols, cellular networks, 5G, etc.

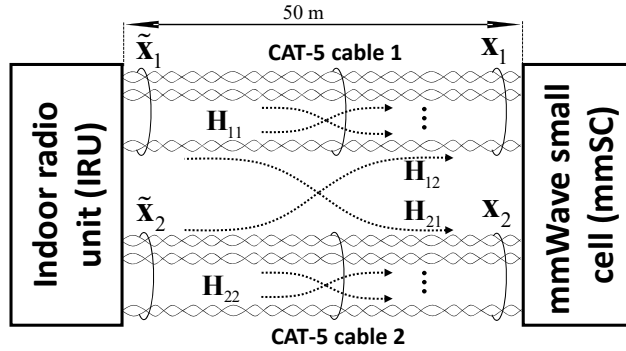


Fig. 9. Cable binder with 2 CAT-5 LAN cables connected between IRU and mmSC.

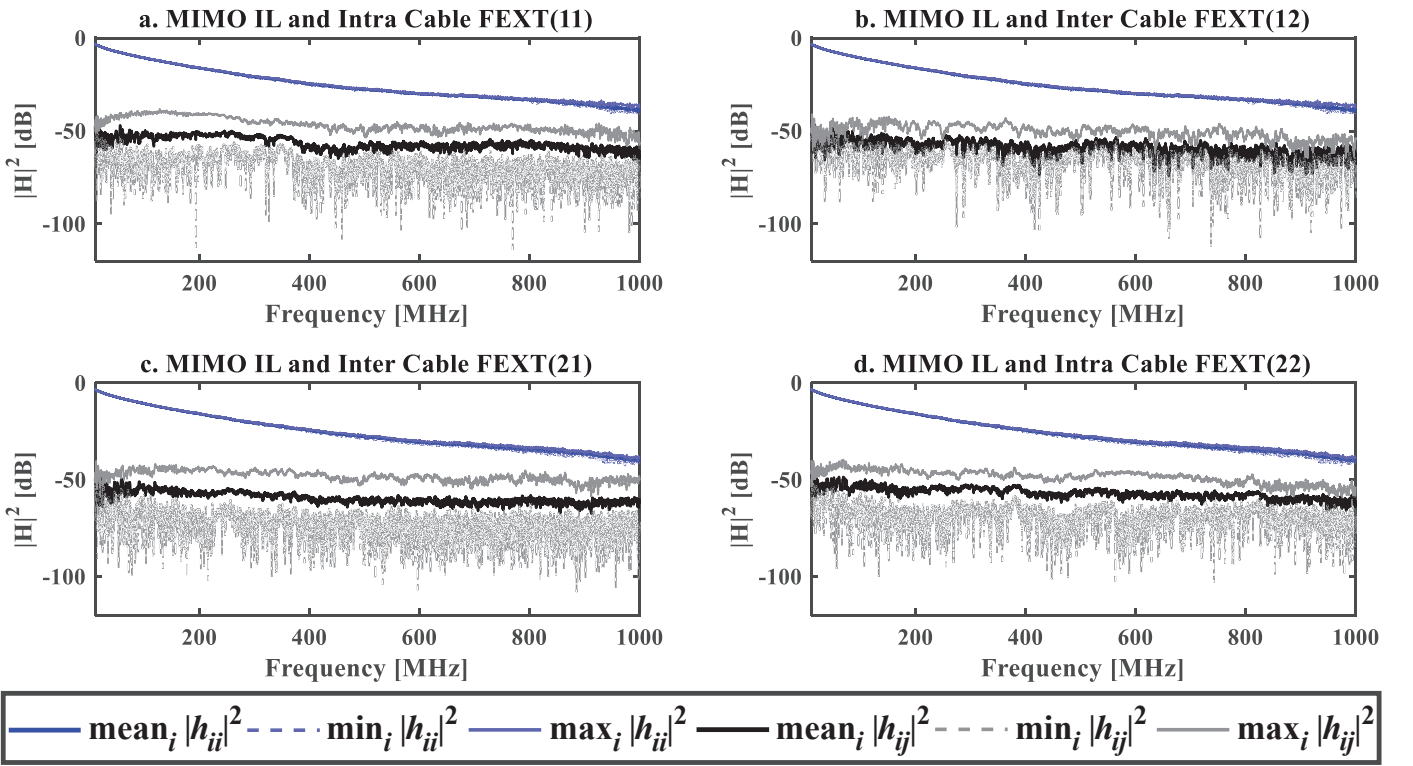


Fig. 10. IL Vs FEXT for Cable binder with 2 CAT-5 LAN cables of 50m length.